Brain microstructural properties related to subjective well-being: diffusion tensor imaging analysis

Running title: Subjective well-being & mean diffusivity

Chiaki Terao Maeda[a], Hikaru Takeuchi[b], Rui Nouchi[c,d], Ryoichi Yokoyama[e], Yuka Kotozaki[f], Seishu Nakagawa[g,h], Atsushi Sekiguchi[i,j], Kunio Iizuka[k], Sugiko Hanawa[g], Tsuyoshi Araki[l], Carlos Makoto Miyauchi[m], Kohei Sakaki[m], Takayuki Nozawa[n], Shigeyuki Ikeda[o], Susumu Yokota[p], Daniele Magistro[q], Yuko Sassa[b], Yasuyuki Taki[a,b,j], Ryuta Kawashima[b,g,m]

[a]*Department of Nuclear Medicine and Radiology, Institute of Development, Aging and Cancer, Tohoku University, Sendai, Japan*

[b]*Division of Developmental Cognitive Neuroscience, Institute of Development, Aging and Cancer, Tohoku University, Sendai, Japan*

[c]*Department of Cognitive Health Science, Institute of Development, Aging, and Cancer (IDAC), Tohoku University, Sendai, Japan*

[d]*Smart Aging Research Center, Tohoku University, Sendai, Japan*

[e]*Suwa Red Cross Hospital, Nagano, Japan*

[f]*Division of Clinical research, Medical-Industry Translational Research Center, Fukushima Medical University School of Medicine, Fukushima, Japan*

[g]*Department of Human Brain Science, Institute of Development, Aging and Cancer Tohoku University, Sendai, Japan*

[h]*Division of Psychiatry, Tohoku Medical and Pharmaceutical University, Sendai, Japan*

[i]*Department of Behavioral Medicine National Institute of Mental Health, National*

Center of Neurology and Psychiatry, Tokyo, Japan

[j]*Division of Medical Neuroimaging Analysis, Department of Community Medical Supports, Tohoku Medical Megabank Organization, Tohoku University, Sendai, Japan*

[k]*Department of Psychiatry Tohoku University Graduate School of Medicine, Sendai, Japan*

[l]*ADVANTAGE Risk Management Co., Ltd, Tokyo, Japan*

[m]*Department of Advanced Brain Science, Institute of Development, Aging and Cancer Tohoku University, Sendai, Japan*

[n]*Research Institute for the Earth Inclusive Sensing, Tokyo Institute of Technology, Tokyo, Japan*

[o]*Department of Ubiquitous Sensing, Institute of Development, Aging and Cancer Tohoku University, Sendai, Japan*

[p]*Faculty of arts and science, Kyushu University, Fukuoka, Japan*

[q]*Department of Sport Science, School of Science and Technology Nottingham Trent University, Nottingham, UK*

Corresponding author:

Chiaki Terao Maeda

Department of Nuclear Medicine and Radiology, Institute of Development, Aging and Cancer, Tohoku University, Sendai, Japan

4-1 Seiryo-cho, Aoba-ku, Sendai 980-8575, Japan

Tel/Fax: +81-22-717-8556

E-mail: chiaki.terao.d3@tohoku.ac.jp

Abstract

Although it is known that health is not merely the absence of disease, the positive aspects of mental health have been less comprehensively researched compared with its negative aspects. Subjective well-being is one of the indicators of positive psychology, and high subjective well-being is considered to benefit individuals in multiple ways. However, the neural mechanisms underlying individual differences in subjective well-being remain unclear, particularly in terms of brain microstructural properties as detected by diffusion tensor imaging. The present study aimed to investigate the relationship between measurements of diffusion tensor imaging (mean diffusivity and fractional anisotropy) and the degree of subjective well-being as measured using a questionnaire. Voxel-based analysis was used to investigate the association between mean diffusivity and subjective well-being scores in healthy young adults (age, 20.7 ± 1.8 years; 695 males and 514 females). Higher levels of subjective well-being were found to be associated with lower mean diffusivity in areas surrounding the right putamen, insula, globus pallidus, thalamus, and caudate. These results indicated that individual subjective well-being is associated with variability in brain microstructural properties.

Key words: subjective well-being, mean diffusivity, diffusion tensor imaging, dopaminergic system, motivation

Introduction

Every person hopes to lead a healthy life. Health is defined by the World Health Organization (WHO) as a state of complete physical, mental, and social well-being and not merely the absence of disease or infirmity. Although this statement defines health as more than a lack of illness, neuropsychological investigations conducted of positive mental health have been fewer than those of psychological disorders and diseases.

Subjective well-being and its components

Subjective well-being (SWB) is an indicator of positive psychology as well as happiness, life satisfaction, and positive social influence (Sell and Nagpal, 1992). SWB is a broad category of phenomena that includes people's emotional responses, domain satisfactions, and global judgments of life satisfaction (Diener *et al.*, 1999). SWB is considered to have pleasant and unpleasant affective features and a cognitive aspect of life satisfaction (Diener and Suh, 1997). Numerous previous studies have suggested that positive affect (PA) and negative affect (NA) are moderately inversely correlated; however, they are perceived as distinct dimensions rather than opposite ends of the same dimension (Headey *et al.*, 1984; Diener *et al.*, 1999; Dodge *et al.*, 2012). According to previous research regarding SWB among patients with psychiatric disorders and nonclinical participants, the correlation between PA and NA was relatively high in patients, and low in nonclinical participants (Ono *et al.*, 1996). Because a decrease in NA does not necessarily promote an increase in PA, it appears to be important to consider PA and NA separately when investigating SWB.

Association between SWB and dopaminergic system

Previous neuropsychological studies have indicated that the dopaminergic system, including striatal areas, contributes to SWB. For instance, antipsychotic medications reduce SWB in patients with psychotic disorders (Haan et al., 2000; Bressan et al., 2002; Mizrahi et al., 2007). These drugs occupy the dopamine D2-receptor, resulting in a reduction of dopaminergic neurotransmission and suppression of psychotic symptoms (Seeman, 2002). Furthermore, blocking of dopamine receptors is associated with reduced motivation and emotional experiences based on natural rewards—processes related to endogenous dopaminergic activity (Kapur *et al.*, 2005)—and could be associated with a reduction in SWB. Other studies have observed subjective happiness scores to decrease in healthy subjects with acute dopamine depletion by alpha-methyl paratyrosine (AMPT) (Fujita et al., 2000; Verhoeff et al., 2001).

Previous neuroimaging studies of SWB

Previous structural magnetic resonance imaging (MRI) studies demonstrated an association between SWB and various brain regions. One study showed that subjective happiness was positively associated with the regional gray matter volume (rGMV) in the rostral anterior cingulate cortex (Matsunaga *et al.*, 2016), whereas another study showed that it was positively associated with the rGMV in the precuneus (Sato *et al.*, 2015). Another study showed that an individual's life satisfaction was positively correlated with the rGMV in the parahippocampal gyrus, and negatively correlated with the rGMV in the precuneus and ventromedial prefrontal cortex (Kong et al., 2015). These discrepancies may be derived from the differences in factors that are associated with SWB depending on the participants' culture and context in which they live, or the relatively small sample size of each study. As for functional MRI, there are growing

findings from resting-state MRI studies using self-report assessment of SWB indicating importance of the default mode network, and emotional and rewarding system (Luo *et al.*, 2014; Shi *et al.*, 2018). We believe that further studies from diverse areas should be conducted on this topic. Accordingly, there are accumulating neuroimaging studies of SWB; however, to the best of our knowledge, studies examining the association between SWB and brain microstructural properties as detected by diffusion tensor imaging (DTI) are scarce.

DTI measures and individual differences

DTI is a MRI technique that exploits the differences in the molecular diffusion of water according to tissue architecture (Basser *et al.*, 1994), including the molecular diffusion rate, directional preference of diffusion, and axial and radial diffusivity (Basser et al., 1994; Basser and Pierpaoli, 1996; Le Bihan et al., 2001). There are two popular measures of DTI—Fractional anisotropy (FA) and Mean diffusivity (MD). FA, the most common index of DTI, is used to represent the motional anisotropy of water molecules, being sensitive to the presence and integrity of white matter (WM) (Assaf and Pasternak, 2008), whereas MD is a scalar measure of the directionally averaged diffusion magnitude and is related to brain tissue integrity (Pierpaoli et al., 1996). Compared with FA, MD can be used to assess the microstructural properties of broader brain structures, including gray matter.

In recent years, differences in MD have been shown to underlie individual cognitive differences and brain pathology (Laricchiuta et al., 2014; Piras et al., 2010). In particular, MD in areas strongly related to the dopaminergic system, particularly subcortical areas including the basal ganglia (globus pallidus, putamen and caudate nucleus) and

thalamus is reportedly associated with several conditions related to differences or changes of the dopaminergic system (Takeuchi & Kawashima, 2018). In our previous study, MD in such areas was robustly associated with some mood states, temperaments and cognitive functions related to dopaminergic function; it was suggested that an overlap of these correlates involved a motivational component (Takeuchi *et al*., 2015). Considering previous findings that the dopaminergic system contributes to SWB (Haan et al., 2000; Mizrahi *et al.*, 2007; Verhoeff et al., 2001), we hypothesized that SWB might be related to MD in the regions associated with the dopaminergic system.

In the present study, we aimed to investigate the relationship between SWB and DTI measures and to test the hypothesis of the association between SWB and MD, particularly MD in the regions associated with the dopaminergic system, using data from a large sample of healthy young adults. Accordingly, we used the Japanese version of the subjective well-being inventory (SUBI) and investigated the relationship between SUBI scores and DTI measures (MD or FA) via voxel-based analysis. Further, we investigated the association between SWB and the motivational state as measured by the Profile of Mood States (POMS) because motivational component is considered to play an important role in the MD in the regions associated with the dopaminergic system.

Methods

Participants

Overall, 1,209 healthy, right-handed individuals (695 males and 514 females) participated in the present study. This research was a part of our ongoing project to

investigate associations among brain imaging results, cognitive function, aging, genetics, and daily habits. Mean participant age was 20.7 years [standard deviation (SD), 1.78; range: 18–27 years]. All participants were university students, postgraduates, or university graduates of <1 year. Each participant had normal vision and none had a history of neurological or psychiatric illness. Handedness was evaluated using the Edinburgh Handedness Inventory (Oldfield, 1971). Written informed consent was obtained from each participant for projects in which they participated. The procedures for all studies were approved by the Ethics Committee of Tohoku University.

Psychological measurements

Subjective well-being inventory

SWB can be quantified using the WHO-SUBI (Sell and Nagpal 1992). SUBI is a self-report questionnaire used to comprehensively assess the degree of an individual's physical, mental, and social well-being based on their own experiences. This questionnaire enables the measurement of two types of SWB independently: PA, an index of psychological healthfulness; and NA, an index of poor psychological healthfulness. SUBI questionnaire comprises 40 items, each rated on a 3-point scale. The items are divided into 11 subscales: sense of satisfaction (F1), sense of achievement (F2), self-confidence (F3), sense of happiness (F4), support of close relatives (F5), social support (F6), family relationships (F7), sense of spiritual control (F8), sense of physical ill health (F9), dissatisfaction with social ties (F10), and sense of disappointment (F11). PA comprises 19 items included in subscales F1 to F7, and NA comprises 21 items included in subscales F7 to F11. Because extremely few of the study

participants had a spouse or children, three questions regarding family relationships (F7) were excluded. Subsequently, 37 items (18 items for PA and 19 for NA) divided into 10 subscales (from F1 to F6 for PA and from F8 to F11 for NA) remained. Examples of the questions associated with PA are "Do you feel your life is interesting?" and "Do you think that most of the members of your family feel closely attached to one another?" Each item was answered using a 3-point scale as follows: 3 = "I strongly agree," 2 = "I somewhat agree," and 1 = "I disagree." Examples of the questions associated with NA are "Do you feel your life is boring?" and "Do you get easily upset if things don't turn out as expected?" Each item is answered using 3-point scale as follows: 1 = "I strongly agree," 2 = "I somewhat agree," and 3 = "I disagree." For both PA and NA, higher scores on each item indicate a better state of well-being. The reliability and validity of this scale has previously been demonstrated (Tonan *et al*., 1995); the internal consistency of PA and NA, as measured with Cronbach's coefficient α, were >0.8 (Ono and Yoshimura, 2010), indicating that the questionnaire was extremely reliable. The correlation coefficients between the 12-Item General Health Questionnaire (Goldberg and Williams, 1988) and both PA and NA were r = −0.43 and r = −0.57, respectively (Ono and Yoshimura, 2010),suggesting that the questionnaire was valid. Additionally, the SUBI questionnaire has previously been used to investigate the SWB of patients (Noguchi et al., 2006; Fujisawa et al., 2010; Iwamoto et al., 2011) and nonclinical participants (Kanai et al., 2016; Sano et al., 2018).

Raven's Advanced Progressive Matrix

The Raven's Advanced Progressive Matrix (RAPM; Raven, 2000), a widely used measure of general intelligence (Melby-Lervåg and Hulme, 2013), was applied to

examine the effects of general intelligence on brain structures to exclude the possibility that the significant correlation between MD and SUBI scores was owing to either an association between the SUBI scores and general intelligence or an association between MD and general intelligence.

Profile of Mood States

POMS (McNair *et al.*, 1992), a measure widely used for the assessment of mood states, was used in the present study. The shortened Japanese version (Yokoyama, 2005) of POMS was adjusted to examine the effect of mood states in the week preceding the use of SUBI questionnaire for each participant. The questionnaire comprised six subscales—tension/anxiety, depression/dejection, anger/hostility, vigor/activity (V/A), fatigue/inertia, and confusion/bewilderment—each consisting of five items. Data for these measures were collected from 1,193 study participants (data from 16 participants were missing). The validity of this measure has previously been demonstrated (Yokoyama 2005); the high reliability of this measure was confirmed in a previous study conducted in our laboratory that included data from the same participants (Takeuc*hi et al*., 2017).

We did not include scales of this measure as covariates in the whole brain imaging analyses because we assumed that SWB would be fundamentally shared by the components of mood states; therefore, these effects were not regressed in the present study. Our previous study investigated the association between POMS and MD (Takeuchi *et al.*, 2017); we adopted this measure in the present study to complement the discussion of the main results.

Behavioral data analysis

The behavioral data were analyzed using the IBM SPSS Statistics 21.0 software package (IBM Corp.; Armonk, NY, USA). Differences between males and females in age and psychological measure scores were analyzed using Mann–Whitney U-tests. In each analysis, p-value of <0.05 was considered significant. The potential association between PA and NA was investigated using multiple regression analysis with age and sex as covariates; a result with a threshold of p-value of <0.05 was considered significant. Moreover, the associations between each SUBI score and other psychological measures were assessed using multiple regression analyses. In each analysis, the dependent variable was the score of PA or NA and the independent variables comprised one of the scores of the POMS or RAPM subscales, age, and sex. These multiple regression analyses of PA and NA were separately performed because correcting one with the other may be inappropriate owing to multicollinearity. In these analyses, results with a threshold p-value of < 0.05 were considered significant after correcting for the false discovery rate (FDR) using the classical one-stage method (Benjamini and Hochberg, 2000).

Image acquisition and analysis

All MRI data were acquired using a 3T Philips Achieva scanner (Philips Medical Systems, Best, Netherlands). Diffusion-weighted data were acquired using a spin-echo echo-planar imaging (EPI) sequence [repetition time (TR) = 10,293 ms, echo time (TE) = 55 ms, field of view (FOV) = 22.4 cm, 2 × 2 × 2 mm^3 voxels, 60 slices, SENSE

reduction factor = 2, number of acquisitions = 1] with an 8-channel head-coil. The diffusion weighting was isotropically distributed along 32 directions (b-value = 1000 s/mm^2). Three images with no diffusion weighting (b-value = 0 s/mm^2) were acquired using a spin-echo EPI sequence (TR = 10,293 ms, TE = 55 ms, FOV = 22.4 cm, 2 × 2 × 2 mm^3 voxels, 60 slices). Acquisitions for phase correction and for signal stabilization were performed; however, they were not used as part of the reconstructed images. FA and MD maps were calculated from the collected images using a commercially available diffusion tensor analysis package (Philips Medical Systems, Best, Netherlands) on the MR console. These procedures involved corrections for motion and distortion caused by eddy currents. All calculations were performed using a previously described method (Le Bih*an et al*., 2001).

Preprocessing of imaging data

Preprocessing of the imaging data was performed using Statistical Parametric Mapping software (SPM8; Wellcome Department of Cognitive Neurology, London, UK) implemented in MATLAB (Mathworks, Natick, MA). We adopted a previously validated two-step new segmentation algorithm (Takeuchi *et al*., 2013) for segmentation of diffusion images. Thereafter, using the diffeomorphic anatomical registration via exponentiated lie algebra (DARTEL) registration process implemented in SPM8, the raw MD map, FA map, GM segmentation map [gray matter concentration (GMC) map], WM segmentation map [white matter concentration (WMC) map], and cerebrospinal fluid (CSF) segmentation map [CSF concentration (CSFC) map] were normalized; the voxel size for all normalized MD (or FA) images and segmented images was 1.5 × 1.5 ×

1.5 mm^3. The template for the DARTEL procedure was created in our previous study, which was developed using participants in the same project (see Takeuchi *et al.*, 2013). Subsequently, from the normalized images of the MD maps, the areas that were least likely to be GM or WM in the averaged normalized GMC and WMC images (defined as "gray matter tissue probability + white matter tissue probability < 0.99") were removed to exclude the strong effects of CSF on MD throughout the analyses. From the normalized images of the FA, the areas that were least likely to be WM (defined as "white matter tissue probability < 0.99") were removed. These images were then smoothed [8 mm full-width at half maximum for MD] and used for second-level analyses. We used SPM8 rather than SPM12 for all preprocessing because all methods and parameters were optimized and validated using SPM8 in our previous study(Takeuchi *et al.*, 2013). For more details of these procedures, see the Supplementary material.

Statistical analysis

Whole brain statistical analysis

The statistical analyses of imaging data were performed using SPM8. We performed multiple regression analyses to assess the relationship between MD or FA and the SUBI scores of PA or NA. The analyses of PA and NA were conducted separately because these scores are regarded as not completely independent, but only partly overlapping, and the correction of both as part of a multiple regression analysis may be inappropriate. Moreover, due to the strength of association between PA and NA, these scores were not analyzed in one multiple regression to avoid multicollinearity. These analyses were performed with sex, age, RAPM score, total intracranial volume (TIV), and PA or NA

scores as covariates. Using the masks created as described above, the analyses for MD were limited to the areas strongly likely to be GM or WM, and those for FA were limited to the areas strongly likely to be WM. Correction for multiple comparisons was performed using threshold-free cluster enhancement (TFCE) (Smith and Nichols, 2009) with randomized nonparametric permutation testing (5000 permutations) using the TFCE toolbox (http://dbm. neuro.uni-jena.de/tfce/). We applied a family-wise error (FWE)-corrected threshold *p*-value of <0.05. We used SPM8 for statistical analyses for compatibility with the software used for permutation-based statistics and the homemade script used for the statistical analyses. The results should not have been affected by the version of SPM used.

Analyses of sex differences in the neural correlates of SUBI scores

We analyzed MD and FA correlates with respect to sex differences because the SUBI scores showed significant differences related to sex in behavioral analyses. Detailed descriptions about the sex differences in the MD and FA correlates of the SUBI scores are presented in the Supplementary material.

Results

Behavioral data

Table 1 shows the mean values and ranges for age and SUBI-PA, SUBI-NA, RAPM, and POMS scores in males and females. Mann–Whitney U-tests showed that females had a significantly higher SUBI score of PA, whereas males had a significantly higher score of NA (i.e., a higher level of SWB). Furthermore, there were significant

differences between males and females in RAPM score and on the subscales of tension/anxiety, depression/dejection, and anger/hostility of POMS. The multiple regression analysis for the association between PA and NA with covariates of age and sex revealed that there was a significant positive correlation ($\beta = 0.410$, $t = 15.525$, $p = 1.090 \times 10^{-49}$) between PA and NA. We noted that because the polarity of NA scores was reversed, both higher PA and NA scores on the SUBI scale are indicative of a better state of well-being. Table 2 and Figure 1 show the distributions of SUBI scores. Figure 2 shows the scatter plot of the association between PA and NA.

No significant correlation was observed between each SUBI score and RAPM score, whereas there were significant correlations between SUBI scores and POMS subscale scores. The results of the association between SUBI and RAPM and that between SUBI and POMS subscales are shown in Table3.

MRI data

Whole brain analyses of the correlations between positive and negative aspects of SUBI and MD

After controlling for age, sex, TIV, and RAPM score, the whole brain multiple regression analysis showed that PA scores were significantly negatively correlated with MD in the anatomical cluster surrounding the right putamen, insula, pallidus, thalamus, caudate, and adjacent areas of WM (Fig 3, Table 4). NA scores were significantly negatively correlated with MD in the anatomical cluster surrounding these same brain regions as well as the middle cingulate gyrus (Fig 3, Table 4). The areas related to the

PA and NA of the SUBI overlapped; however, the area related to the NA was broader than that related to the PA. We noted that both higher PA and NA scores on the SUBI scale indicate a better state of well-being. These analyses did not consider the effects of regional GMC, WMC, and CSFC differences on MD because nonparametric statistical tests were used that did not consider these effects. However, we carefully removed the CSF in the preprocessing stages and additionally performed region of interest (ROI) analyses to consider these effects; the results did not change the conclusions reached. Detailed descriptions of these ROI analyses are presented in the Supplementary material.

Whole brain analyses of the correlations between PA and NA of SUBI and FA

After controlling for age, sex, TIV, and RAPM scores, the whole brain multiple regression analysis showed that NA scores were significantly positively correlated with FA in the anatomical cluster including the anterior internal capsule (Fig 4, Table 5). No significant correlations were observed between PA scores and FA.

Discussion

To the best of our knowledge, this is the first study that investigates the relationship between DTI measurements (MD and FA) and SWB. We demonstrated—for the first time—that a higher SUBI-PA score, indicative of a higher level of SWB, was significantly associated with a lower MD of brain areas surrounding the right putamen, globus pallidus, insula, caudate, and thalamus. Similarly, a higher SUBI-NA score, indicative of a higher level of SWB, was associated with lower MD of the same areas,

as well as the middle cingulate gyrus. Consistent with our hypothesis, the areas in which MD significantly correlated with SWB were associated with the dopaminergic system. Dopaminergic neurons located in the substantia nigra pars compacta (SNc) project into the striatum, creating the nigrostriatal dopaminergic system (Ungerstedt, 1971). The nigrostriatal dopaminergic system is primarily associated with motor function, as the degeneration of this pathway is reportedly a primary pathological feature of Parkinson's disease (Sean *et al.*, 1965). Additionally, accumulating evidence implies the involvement of the nigrostriatal dopaminergic system in reward and motivation, which have long been identified as the roles of the mesolimbic dopaminergic system (Wise, 2009). Recently, dopaminergic dysfunction in schizophrenia was determined to be the greatest within nigrostriatal pathways and that dysfunction appeared fundamental to the mechanisms underlying those symptoms (McCutche*on et al.*, 2019). The globus pallidus receives a dopaminergic input from the substantia nigra (Lindvall and Björklund, 1979) and is thus an important part of the dopaminergic circuitry. Indeed, dopamine reverses reward insensitivity in patients with apathy following globus pallidus lesions (Adam *et al.*, 2013). Previous studies using autoradiography and positron emission tomography (PET) have shown that the thalamus contains a high density of dopamine D2 receptors (Hall *et al.*, 1996; Farde *et al.*, 1997). The thalamus is a part of the corticobasal ganglia circuitry, which has been considered to comprise anatomically and functionally segregated subcircuits including motor, cognitive, and emotional domains (Alexander, 1986), as well as exhibits an integrative function for the domains of the circuitry (Haber and Calzavara, 2009). Previous studies have suggested that DA signaling is involved in key neurochemical mechanisms of the insular, striatal and prefrontal regions that cause individual differences in cost/benefit decision-making

(Treadway *et al.*, 2012). The insula is important for motivation and dysfunction and may be linked to motivational deficits in individuals with anhedonia (Namkung *et al.*, 2017). Higher NA scores were associated with lower MD in the middle and posterior cingulate cortex, which commonly plays a role in reward processing (Liu *et al.*, 2011). Accordingly, MD of clusters surrounding all these areas may be associated with SWB via dopaminergic system.

As described above, MD is a measure of the directionally averaged magnitude of water diffusion (Pierpaoli et al., 1996; Pierpaoli et al., 2001; Le Bihan et al., 2001). Larger spaces between obstacles such as neurons, glial cells, and blood vessels should facilitate water diffusion more freely and cause an increase in MD; by contrast, smaller spaces, such as those that arise when cells or blood vessels increase in size or number or when tissue organization is enhanced, prevent water diffusion, thereby decreasing MD (Sagi et al., 2012; Johansen-Berg et al., 2012). As mentioned in previous studies (Nakagawa et al., 2016; Nakagawa et al., 2017), there is a significant negative correlation between dopamine synthesis capacity and MD in the striatum (Kawaguchi *et al*., 2014).

MD in areas related to the dopaminergic system is reportedly more sensitive in the detection of neuropathology in the dopaminergic system (Péran et al., 2010; Seppi et al., 2004). Compared with healthy individuals, patients with Parkinson's disease displayed higher MD values in the thalamus, striatum, and posterior substantia nigra (Péran et al., 2010; Arribarat et al., 2019). Patients with Parkinson's disease exhibit a range of neuropsychiatric symptoms including depression, anxiety, apathy, fatigue, and psychotic symptoms, as well as the loss of motor control (Aarsland, Marsh, & Schrag, 2009; Aarsland et al., 1999). The impairment of dopaminergic system might be associated with higher MD values and affective disorders. Additionally, this can support the

possibility of an association of the dopaminergic system with the negative correlation between MD and SWB observed in the present study.

Previous studies of healthy participants from our research group have revealed an association between MD of subcortical areas and individual traits and states (for review, see Takeuchi & Kawashima, 2018). It was demonstrated that only the motivational state (V/A) was negatively correlated with MD in the right-sided areas including the globus pallidus, putamen, posterior insula, caudate body, and thalamus, whereas the other mood subscales of POMS showed no significant relationships with MD in the whole brain analyses (Takeuchi *et al*., 2017). The present study results showed that both PA and NA were negatively correlated with MD in these overlapping areas. Additionally, MD in the globus pallidus was found to be associated with some cognitive functions (verbal creativity measured by divergent thinking) and multiple personalities in the Temperament and Character Inventory; the motivational factor may be the key component linking these associations (Takeuchi *et al.*, 2015). Degrees of fatigue were associated with higher MD values in the basal ganglia (Nakagawa *et al.*, 2016) and disruption of the dopaminergic system was proposed as a common mechanism underlying fatigue (Lorist *et al.*, 2009). Furthermore, it has been suggested that motivation is involved in this association (Nakagawa *et al.*, 2016). In reviewing previous findings, decreased MD values in areas highlighted in the present study appears to be associated with a facilitated motivational state of dopaminergic function in healthy participants (Takeuchi and Kawashima, 2018). The present behavioral results that both PA and NA scores were significantly correlated with V/A score from POMS might support this notion, although there were significant correlations between SUBI scores and of the remaining subscales of POMS. Additional thorough investigations are

required in the future to identify underlying neural mechanisms of those correlations.

In addition, a higher SUBI-NA score, which was consistent with a higher level of SWB, was associated with higher FA of the right anterior internal capsule. The anterior internal capsule is adjacent to the striatum and contains fibers connecting the subcortical nuclei and frontal cortex (Alexander *et al.*, 1986; Alexander *et al.*, 1991; Axer and Keyserlingk, 2000). Fronto–thalamic–striatal connectivity is important for the appreciation of reward, emotional processing, and mood state (Sussmann *et al.*, 2009). Moreover, it has been suggested that disturbed frontosubcortical connectivity is a key factor in psychopathology (Mega and Cummings, 1994). Decreased integrity in the structural connections of the frontal lobe and subcortical structures may be associated with lower SWB.

In the present study, the right-sided areas, including the basal ganglia, thalamus and insula specifically showed negative correlation with SWB. This is consistent with the right hemisphere hypothesis, which assumes a general dominance of the right hemisphere for all emotions, regardless of affective valence (Boro*d et al*., 1998; Ross, 1984). Moreover, some previous studies investigating the laterality of the dopaminergic dysfunction in Parkinson's disease suggested that the right basal ganglia plays a greater role in affective processes than the left (Péron *et al.*, 2017; Stirnimann *et al.*, 2018). Based on these findings, the right-sided areas observed in the present study may be associated with a greater role in emotional processing. Numerous previous studies have focused on the association between approach/avoidance motivation and hemispheric asymmetry; therefore, the left hemisphere may play a role in approach-related affect, whereas the right hemisphere may play a role in avoidance-related affect (Sutton and Davidson, 1997; Harmon-Jones et al., 2010). Recently, this asymmetric pattern related

to approach/avoidance was identified in the striatal dopamine function (Porat *et al.*, 2014; Aberg *et al.*, 2015). Considering that the result of the present study indicated SWB can be positively associated with the right striatal dopaminergic function, individuals with lower SWB may have poorer capabilities to avoid emotionally negative stimuli.

Significant differences between males and females were observed in SUBI-PA and SUBI-NA scores. Females showed significantly higher PA scores, which were associated with better states of SWB; conversely, males exhibited significantly higher NA scores, which were associated with lesser subjective ill-being states (as well as indicating better states of SWB). The mechanisms underlying these sex differences in SWB remain unclear. Previous research regarding SWB has not provided consistent evidence concerning sex differences (see Batz-Barbarich and Tay, 2018). Moreover, it appears that sex differences in SWB are often small, not universal, and depend on the cultural values and societal conditions (Diener, Lucas, *et al.*, 2018). However, based on the components of PA and NA, previous large scale, nationally representative studies have provided some findings regarding sex differences. Younger females tended to have higher levels of happiness than younger males, whereas older females have lower levels of happiness than older males(Inglehart, 2002; Easterlin, 2003). A large-scale research study using data from the Gallup World Poll showed that females exhibited higher levels of negative emotion (lower levels of SWB) than males (Zuckerman *et al.*, 2017). Behavioral data in the present study appears to be consistent with these previous findings. Moreover, the comparison of behavioral data in the present study was consistent with the results of a previous study involving an older study population (1,618 Japanese participants; age range 20-64 years; male mean age: 46.4 years, female

mean age: 46.9 years); that study showed that males had significantly higher PA and NA SUBI scores (Ono and Yoshimura, 2010).

The current study has several limitations that should be noted. First, because this study used a cross-sectional design, the results cannot determine a causal relationship between SWB and MD. To overcome this limitation, a prospective study that confirms such causality is required. Second, the study included young healthy participants who possessed high educational backgrounds. Because previous reviews have suggested that several life circumstances, including, marriage, widowhood, unemployment and disability affected SWB (Larsen and Eid, 2008; Diener, Oishi, *et al.*, 2018), our findings cannot be generalized for the entire human population. A larger and more representative sample set is required for such generalization. Third, dopamine was not measured in the present study; thus, future investigations should include more sensitive measures of dopamine function such as PET scans. It should be noted that there is a possibility that neural changes other than those of dopaminergic neurons may affect MD in areas related to the dopaminergic system. For example, previous studies investigating patients with Huntington's disease, which is characterized by the degeneration of cholinergic and GABAergic neurons in the striatum, found that while dopaminergic neurons are relatively unaffected, MD was increased in areas around the striatum compared with healthy control (Douau*d et al.*, 2009; Sánchez-Castañeda *et al.*, 2013).

In conclusion, the present study is the first to reveal the association between SWB and microstructural properties using DTI. The results showed that individual measurements of SWB are reflected in the variability of the microstructural properties of brain areas involved in the dopaminergic function. Our findings integrate the psychological and physiological aspects of SWB using neuroimaging techniques, and advance our

understanding of the contribution of our brains to SWB. Our results suggest the possibility of enhancing well-being via physiological changes in the brain.

Acknowledgments

We respectfully thank Yuki Yamada for operating the MRI scanner, Yuriko Suzuki from Philips for advice on diffusion-weighted imaging, and Haruka Nouchi for being an examiner of psychological tests. We also thank study participants, the other examiners of psychological tests, and all of our colleagues in Institute of Development, Aging and Cancer and in Tohoku University for their support. The authors would like to thank Enago (http://www.enago.jp) for the English language review.

Funding

This study was supported by a Grant-in-Aid for Young Scientists (B) (KAKENHI 23700306) and a Grant-in-Aid for Young Scientists (A) (KAKENHI 25700012) from the Ministry of Education, Culture, Sports, Science, and Technology.

Conflicts of interest

The authors declare no conflicts of interest.

References

Aarsland, D., Larsen, J.P., Lim, N.G., et al. (1999). Range of neuropsychiatric disturbances in patients with Parkinson's disease. *Journal of Neurology Neurosurgery and Psychiatry*, **67**, 492–96

Aarsland, D., Marsh, L., Schrag, A. (2009). Neuropsychiatric symptoms in Parkinson's disease. *Movement Disorders*, **24**, 2175–86

Aberg, K.C., Doell, K.C., Schwartz, S. (2015). Hemispheric asymmetries in striatal reward responses relate to approach–avoidance learning and encoding of positive–negative prediction errors in dopaminergic midbrain regions. *Journal of Neuroscience*, **35**, 14491–500

Adam, R., Leff, A., Sinha, N., et al. (2013). Dopamine reverses reward insensitivity in apathy following globus pallidus lesions. *Cortex*, **49**, 1292–1303
Alexander, G. (1986). Parallel Organization of Functionally Segregated Circuits Linking Basal Ganglia and Cortex. *Annual Review of Neuroscience*, **9**, 357–81
Alexander, G.E., Crutcher, M.D., DeLong, M.R. (1991). Basal ganglia-thalamocortical circuits: parallel substrates for motor, oculomotor, "prefrontal" and "limbic" functions. *Progress in brain research*, **85**, 119–46
Alexander, G.E., DeLong, M.R., Strick, P.L. (1986). Parallel organization of functionally segregated circuits linking basal ganglia and cortex. *Annual review of neuroscience*, **9**, 357–81
Arribarat, G., Pasternak, O., De Barros, A., et al. (2019). Substantia nigra locations of iron-content, free-water and mean diffusivity abnormalities in moderate stage Parkinson's disease. *Parkinsonism and Related Disorders*, **65**, 146–52
Assaf, Y., Pasternak, O. (2008). Diffusion Tensor Imaging (DTI) -based White Matter Mapping in Brain Research : A Review. *Journal of Molecular Neuroscience*, **34**, 51–61
Axer, H., Keyserlingk, D.G. V. (2000). Mapping of fiber orientation in human internal capsule by means of polarized light and confocal scanning laser microscopy. *Journal of Neuroscience Methods*, **94**, 165–75
Basser, P.J., Mattiello, J., Lebihan, D. (1994). MR Diffusion Tensor Spectroscopy and Imaging. *Biophysical Journal*, **66**, 259–67
Basser, P.J., Pierpaoli, C. (1996). Microstructural and physiological features of tissues elucidated by quantitative-diffusion-tensor MRI. *Journal of Magnetic Resonance - Series B*, **111**, 209–19
Batz-Barbarich, C., Tay, L. (2018). Gender Differences in Subjective Well-Being. In: *Handbook of well-being*. Salt Lake City: DEF Publishers.
Benjamini, Y., Hochberg, Y. (2000). On the Adaptive Control of the False Discovery Rate in Multiple Testing With Independent Statistics. *Journal of Educational and Behavioral Statistics*, **25**, 60–83
Le Bihan, D., Mangin, J., Poupon, C., et al. (2001). Diffusion tensor imaging: Concepts and applications. *Journal of magnetic resonance imaging*, **13**, 534–46
Borod, J.C., Obler, L.K., Erhan, H.M., et al. (1998). Right hemisphere emotional perception: Evidence across multiple channels. *Neuropsychology*, **12**, 446–58
Bressan, R.A., Costa, D.C., Jones, H.M., et al. (2002). Typical antipsychotic drugs - D2 receptor occupancy and depressive symptoms in schizophrenia. *Schizophrenia Research*, **56**, 31–36
Diener, E., Lucas, R.E., Oishi, S. (2018). Advances and Open Questions in the Science of Subjective Well-Being. *Collabra Psychol*, **4**, 1–78
Diener, E., Oishi, S., Tay, L. (2018). Advances in subjective well-being research. *Nature Human Behaviour*, **2**, 253–60
Diener, E., Suh, E. (1997). Measuring quality of life: Economic, social, and subjective indicators. *Social Indicators Research*, **40**, 189–216
Diener, E., Suh, E.M., Lucas, R.E., et al. (1999). Subjective Weil-Being : Three Decades of Progress. *Psychological Bulletin*, **125**, 276–302
Dodge, R., Daly, A.P., Huyton, J., et al. (2012). The challenge of defining wellbeing. *International Journal of Wellbeing*, **2**, 222–35
Douaud, G., Behrens, T.E., Poupon, C., et al. (2009). In vivo evidence for the selective

subcortical degeneration in Huntington's disease. *NeuroImage*, **46**, 958–66
Easterlin, R.A. (2003). Happiness of Women and Men in Later Life: Nature, Determinants, and Prospects. In: *Advances in quality-of-life theory and research*. Dordrecht: Kluwer Academic, p. 13–26.
Farde, L., Suhara, T., Nyberg, S., et al. (1997). A PET-study of [11C]FLB 457 binding to extrastriatal D2-dopamine receptors in healthy subjects and antipsychotic drug-treated patients. *Psychopharmacology*, **133**, 396–404
Fujisawa, D., Nakagawa, A., Tajima, M., et al. (2010). Cognitive behavioral therapy for depression among adults in Japanese clinical settings : a single-group study. *BMC Research Notes*, **3**
Fujita, M., Verhoeff, N.P.L.G., Varrone, A., et al. (2000). Imaging extrastriatal dopamine D2 receptor occupancy by endogenous dopamine in healthy humans. *European Journal of Pharmacology*, **387**, 179–88
Goldberg, D., Williams, P. (1988). *A User's Guide to the General Health Questionnaire*. Windsor: Nfer-Nelson.
Haan, L. de, Lavalaye, J., Linszen, D., et al. (2000). Subjective Experience and Striatal Dopamine D 2 Receptor Occupancy in Patients With Schizophrenia Stabilized by Olanzapine or Risperidone. *American Journal of Psyachiatry*, **157**, 1019–20
Haber, S.N., Calzavara, R. (2009). The cortico-basal ganglia integrative network: the role of the thalamus. *Brain Research Bulletin*, **78**, 69–74
Hall, H., Farde, L., Hallden, C., et al. (1996). Autoradiographic localization of extrastriatal D2-dopamine receptors in the human brain using [125I]epidepride. *Synapse*, **23**, 115–23
Harmon-Jones, E., Gable, P.A., Peterson, C.K. (2010). The role of asymmetric frontal cortical activity in emotion-related phenomena: A review and update. *Biological Psychology*, **84**, 451–62
Headey, B.W., Holmstom, E., Wearing, A.J. (1984). Well-being and ill-being: Different dimensions? *Social Indicators Research*, **14**, 115–39
Inglehart, R. (2002). Gender, aging, and subjective well-being. *International Journal of Comparative Sociology*, **43**, 391–408
Iwamoto, R., Yamawaki, N., Sato, T. (2011). Increased self-transcendence in patients with intractable diseases. *Psychiatry and Clinical Neurosciences*, **65**, 638–47
Johansen-berg, H., Baptista, C.S., Thomas, A.G. (2012). Human Structural Plasticity at Record Speed. *Neuron*, **73**, 1058–60
Kanai, Y., Takaesu, Y., Nakai, Y., et al. (2016). The influence of childhood abuse, adult life events, and affective temperaments on the well-being of the general, nonclinical adult population. *Neuropsychiatric Disease and Treatment*, **12**, 823–32
Kapur, S., Mizrahi, R., Li, M. (2005). From dopamine to salience to psychosis — Linking biology , pharmacology and phenomenology of psychosis. *Schizophrenia Research*, **79**, 59–68
Kawaguchi, H., Obata, T., Takano, H., et al. (2014). Relation between Dopamine Synthesis Capacity and Cell- Level Structure in Human Striatum : A Multi-Modal Study with Positron Emission Tomography and Diffusion Tensor Imaging. *PLoS ONE*, **9**, 1–6
Kong, F., Wang, X., Hu, S., & Liu, J. (2015). Neural correlates of psychological resilience and their relation to life satisfaction in a sample of healthy young adults. Neuroimage, **123**, 165-172.

Laricchiuta, D., Petrosini, L., Piras, F., et al. (2014). Linking novelty seeking and harm avoidance personality traits to basal ganglia : volumetry and mean diffusivity. *Brain Structure and Function*, **219**, 793–803
Larsen, R.J., Eid, M. (2008). Ed Diener and the Science of Subjective Well-Being. In: *The Science of Subjective Well-Being*. New York: Guilford Press.
Lindvall, O., Björklund, A. (1979). Dopaminergic innervation of the globus pallidus by collaterals from the nigrostriatal pathway. *Brain research*, **172**, 169–73
Liu, X., Hairston, J., Schrier, M., & Fan, J. (2011). Common and distinct networks underlying reward valence and processing stages: a meta-analysis of functional neuroimaging studies. *Neuroscience & Biobehavioral Reviews*, **35**, 1219-1236.
Lorist, M.M., Bezdan, E., Caat, M. ten, et al. (2009). The influence of mental fatigue and motivation on neural network dynamics; an EEG coherence study. *Brain Research*, **1270**, 95–106
Luo, Y., Huang, X., Yang, Z., et al. (2014). Regional homogeneity of intrinsic brain activity in happy and unhappy individuals. *PLoS ONE*, **9**, 1–8
Matsunaga, M., Kawamichi, H., Koike, T., et al. (2016). Structural and functional associations of the rostral anterior cingulate cortex with subjective happiness. *NeuroImage*, **134**, 132–41
McCutcheon, R.A., Abi-Dargham, A., Howes, O.D. (2019). Schizophrenia, Dopamine and the Striatum: From Biology to Symptoms. *Trends in neurosciences*, **42**, 205–20
McNair, D., Lorr, M., Droppleman, L. (1992). *Profile of Mood States*. San Diego: Educational and Industrial Testing Service.
Mega, M.S., Cummings, J.L. (1994). Frontal-subcortical circuits and neuropsychiatric disorders. *Journal of Neuropsychiatry and Clinical Neurosciences*, **6**, 358–70
Melby-Lervåg, M., Hulme, C. (2013). Is working memory training effective? A meta-analytic review. *Developmental psychology*, **49**, 270–91
Mizrahi, R., Rusjan, P., Agid, O., et al. (2007). Adverse Subjective Experience With Antipsychotics and Its Relationship to Striatal and Extrastriatal D 2 Receptors : a PET Study in Schizophrenia. *Am J Psychiatry*, **164**, 630–37
Nakagawa, S., Takeuchi, H., Taki, Y., et al. (2016). Basal ganglia correlates of fatigue in young adults. *Scientific Reports*, **6**, 4–10
Nakagawa, S., Takeuchi, H., Taki, Y., et al. (2017). Lenticular nucleus correlates of general self-efficacy in young adults. *Brain Structure and Function*, **222**, 3309–18
Namkung, H., Kim, S., Sawa, A. (2017). The insula: an underestimated brain area in clinical neuroscience, psychiatry, and neurology. *Trends in Neurosciences*, **40**, 200–207
Noguchi, W., Morita, S., Ohno, T., et al. (2006). Spiritual needs in cancer patients and spiritual care based on logotherapy. *Supportive Care in Cancer*, **14**, 65–70
Oldfield, R.C. (1971). The assessment and analysis of handedness: The Edinburgh inventory. *Neuropsychologia*, **9**, 97–113
Ono, Y., Kimio, Y., Keita, Y., et al. (1996). Psychological well-being and ill-being: WHO Subjective Well-being Inventory (SUBI). *The Japanese Journal of Stress Sciense*, **10**, 273–78
Ono, Y., Yoshimura, K. (2010). *Japanese Version of WHO SUBI*. Tokyo: Kanekoshobo.
Péran, P., Cherubini, A., Assogna, F., et al. (2010). Magnetic resonance imaging

markers of Parkinson's disease nigrostriatal signature. *Brain*, **133**, 3423–33
Péron, J., Renaud, O., Haegelen, C., et al. (2017). Vocal emotion decoding in the subthalamic nucleus: An intracranial ERP study in Parkinson's disease. *Brain and Language*, **168**, 1–11
Pierpaoli, C., Barnett, A., Pajevic, S., et al. (2001). Water Diffusion Changes in Wallerian Degeneration and Their Dependence on White Matter Architecture. *NeuroImage*, **13**, 1174–85
Pierpaoli, C., Jezzard, P., Basser, P.J., et al. (1996). Diffusion Tensor MR Imaging of the Human Brain. *Radiology*, **201**, 637–48
Piras, F., Caltagirone, C., Spalletta, G. (2010). Working memory performance and thalamus microstructure in healthy subjects. *Neuroscience*, **171**, 496–505
Porat, O., Hassin-Baer, S., Cohen, O.S., et al. (2014). Asymmetric dopamine loss differentially affects effort to maximize gain or minimize loss. *Cortex*, **51**, 82–91
Raven, J. (2000). The Raven's Progressive Matrices : Change and Stability over Culture and Time. *Cognitive Psychology*, **41**, 1–48
Ross, E.D. (1984). Right hemisphere's role in language, affective behavior and emotion. *Trends in Neurosciences*, **7**, 342–46
Sagi, Y., Tavor, I., Hofstetter, S., et al. (2012). Learning in the Fast Lane : New Insights into Neuroplasticity. *Neuron*, **73**, 1195–1203
Sánchez-Castañeda, C., Cherubini, A., Elifani, F., et al. (2013). Seeking huntington disease biomarkers by multimodal, cross-sectional basal ganglia imaging. *Human Brain Mapping*, **34**, 1625–35
Sano, K., Kawashima, M., Takechi, S., et al. (2018). Exercise program improved subjective dry eye symptoms for office workers. *Clinical Ophthalmology*, **12**, 307–11
Sato, W., Kochiyama, T., Uono, S., et al. (2015). The structural neural substrate of subjective happiness. *Scientific Reports*, **5**, 1–7
Sean, O., Mary, L., Barbara, C. (1965). Dopamine and basal ganglia disorders. *Neurology*, **15**, 980–980
Seeman, P. (2002). Atypical Antipsychotics: Mechanism of Action. *The Canadian Journal of Psychiatry*, **47**, 27–38
Sell, H., Nagpal, R. (1992). *Assessment of Subjective Well-Being. The Subjective Well-Being Inventory (SUBI).* New Delhi: World Health Organizaiton, Regional Office for South-East Asia.
Seppi, K., Schocke, M.F.H., Donnemiller, E., et al. (2004). Comparison of diffusion-weighted imaging and [123I] IBZM-SPECT for the differentiation of patients with the Parkinson variant of multiple system atrophy from those With Parkinson's disease. *Movement Disorders*, **19**, 1438–45
Shi, L., Sun, J., Wu, X., et al. (2018). Brain networks of happiness: Dynamic functional connectivity among the default, cognitive and salience networks relates to subjective well-being. *Social Cognitive and Affective Neuroscience*, **13**, 851–62
Smith, S.M., Nichols, T.E. (2009). Threshold-free cluster enhancement: Addressing problems of smoothing, threshold dependence and localisation in cluster inference. *NeuroImage*, **44**, 83–98
Stirnimann, N., N'Diaye, K., Jeune, F. Le, et al. (2018). Hemispheric specialization of the basal ganglia during vocal emotion decoding: Evidence from asymmetric Parkinson's disease and 18FDG PET. *Neuropsychologia*, **119**, 1–11

Sussmann, J.E., Lymer, G.K.S., Mckirdy, J., et al. (2009). White matter abnormalities in bipolar disorder and schizophrenia detected using diffusion tensor magnetic resonance imaging. *Bipolar Disorders*, **11**, 11–18

Sutton, S.K., Davidson, R.J. (1997). Prefrontal brain asymmetry: A biological substrate of the behavioral approach and inhibition systems. *Psychological Science*, **8**, 204–10

Takeuchi, H., Kawashima, R. (2018). Mean Diffusivity in the Dopaminergic System and Neural Differences Related to Dopaminergic System. *Current Neuropharmacology*, **16**, 460–74

Takeuchi, H., Taki, Y., Sekiguchi, A., et al. (2017). Mean diffusivity of basal ganglia and thalamus specifically associated with motivational states among mood states. *Brain Structure and Function*, **222**, 1027–37

Takeuchi, H., Taki, Y., Sekiguchi, A., et al. (2015). Mean Diffusivity of Globus Pallidus Associated with Verbal Creativity Measured by Divergent Thinking and Creativity-Related Temperaments in Young Healthy Adults. *Human Brain Mapping*, **36**, 1808–27

Takeuchi, H., Taki, Y., Thyreau, B., et al. (2013). White matter structures associated with empathizing and systemizing in young adults. *NeuroImage*, **77**, 222–36

Tonan, K., Sonoda, A., Ono, Y. (1995). Production of The Subjective Well-being Inventory Japanese Edition: It's Reliability and Validity. *The Japanese Journal of Health Psychology*, **8**, 12–19

Treadway, M.T., Buckholtz, J.W., Cowan, R.L., et al. (2012). Dopaminergic Mechanisms of Individual Differences in Human Effort-Based Decision-Making. *The Journal of Neuroscience*, **32**, 6170–76

Ungerstedt, U. (1971). Stereotaxic Mapping of the Monoamine Pathways in the Rat Brain. *Acta Physiologica Scandinavica*, **82**, 1–48

Verhoeff, N.P.L.G., Kapur, S., Hussey, D., et al. (2001). A Simple Method to Measure Baseline Occupancy of Neostriatal Dopamine D 2 Receptors by Dopamine In Vivo in Healthy Subjects. *Neuropsychopharmacology*, **25**, 213–23

Wise, R.A. (2009). Roles for nigrostriatal — not just mesocorticolimbic — dopamine in reward and addiction. *Trends in Neurosciences*, **32**, 517–24

Yokoyama, K. (2005). *POMS Shortened Version (in Japanese)*. Kanekoshobo.

Zuckerman, M., Li, C., Diener, E.F. (2017). Societal conditions and the gender difference in well-being: Testing a three-stage model. *Personality and Social Psychology Bulletin*, **43**, 329–36

Figure legends:

Figure 1. Distribution of SUBI scores. Histograms show the distribution of PA (a) or NA (b) scores.

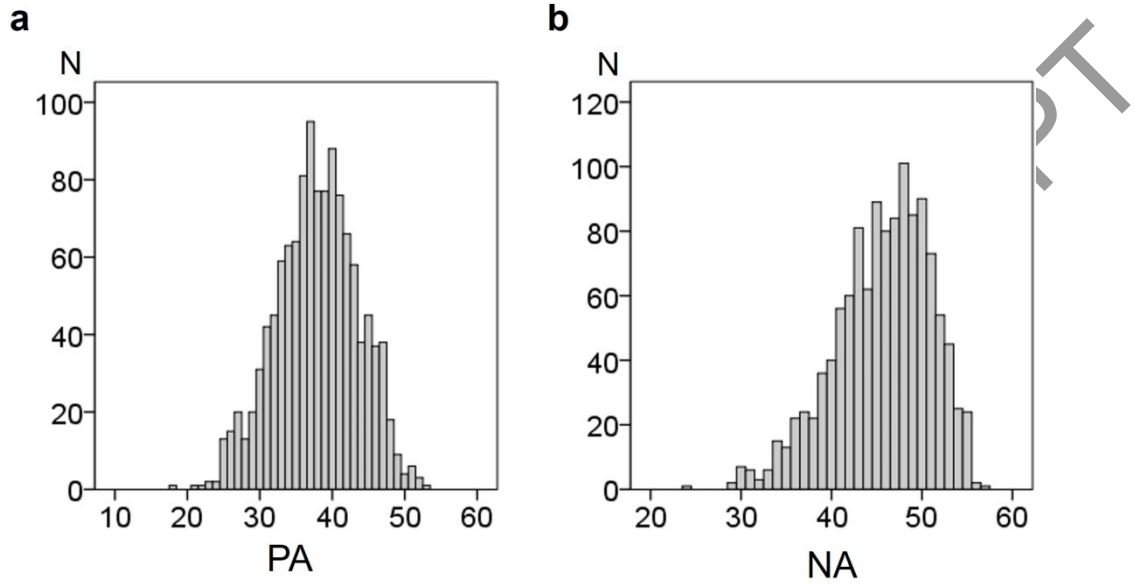

Figure 2. Association between PA and NA. Residual plots with trend lines depict the correlation between residuals of PA and NA in multiple regression analyses with covariates including age and sex.

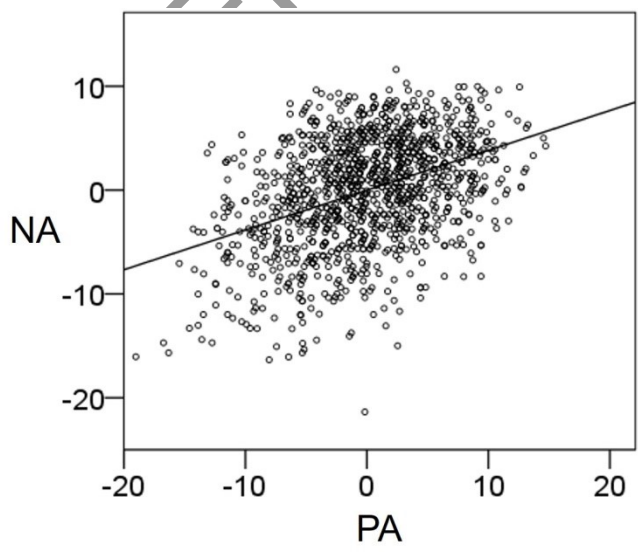

Figure 3. Regions with significant negative correlations between MD and SUBI scores. Results shown were obtained using threshold-free cluster enhancement (TFCE) based on 5,000 permutations ($p < 0.05$). Regions with significant correlations were overlaid on a "single subject" T1 image using SPM8. The color represents the strength of the TFCE value. Regions with significant negative correlations between MD and SUBI-PA scores (a). Regions with significant negative correlations between MD and SUBI-NA scores (b). Residual plots are shown with trend lines depicting the correlations between residuals in each multiple regression analysis using the MD value of each significant peak voxel as a dependent variable and PA (c) or NA (d) scores and other confounding factors as independent variables.

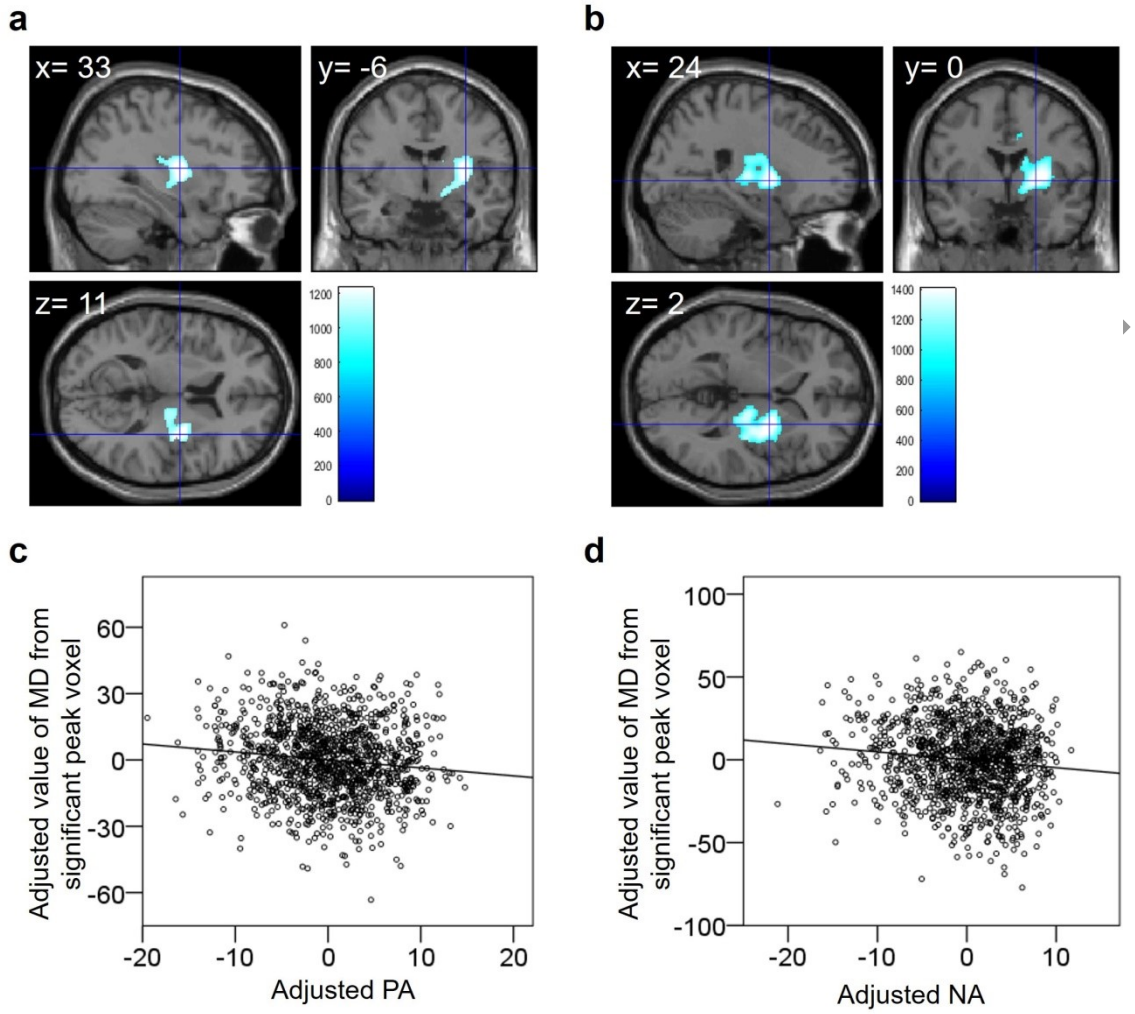

Figure 4. A region with significant negative correlation between FA and SUBI-NA scores. The result shown was obtained using threshold-free cluster enhancement (TFCE) based on 5,000 permutations ($p < 0.05$). Regions with significant correlation were overlaid on a "single subject" T1 image using SPM8. The color represents the strength of the TFCE value (a). A residual plot is shown with a trend line depicting the correlation between residuals in a multiple regression analysis using the FA value of each significant peak voxel as a dependent variable and the NA score and other confounding factors as independent variables (b).

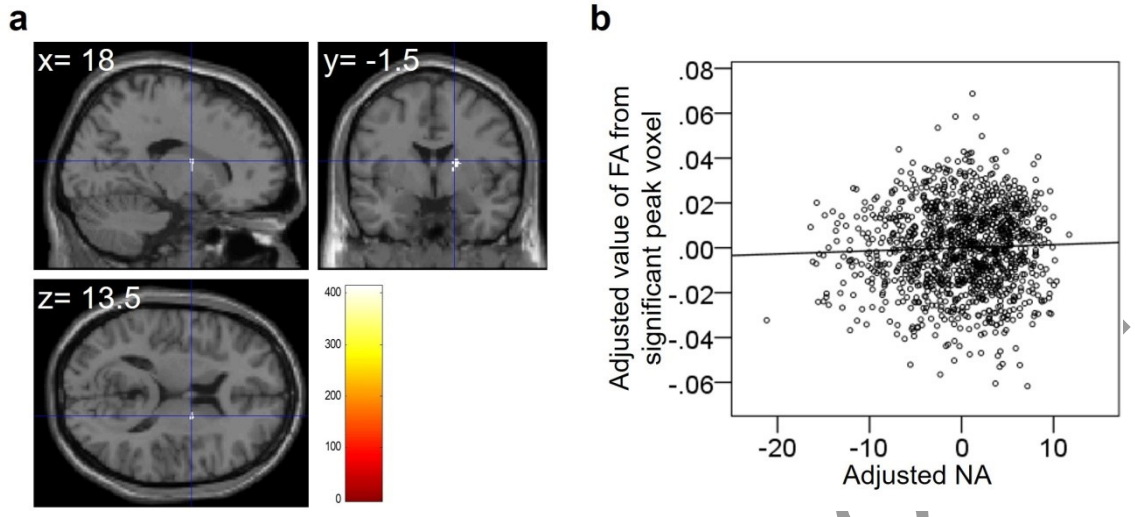

Table 1. Demographic variables of the study participants

		Males		Females		
		Mean	Range	Mean	Range	*p*
Age		20.81	18–27	20.59	18–27	0.272
SUBI[a]	PA[b]	37.44	18–52	38.53	22–53	<0.001*
	NA[c]	45.93	24–55	45.26	29–57	0.038*
RAPM[d]		28.79	13–36	28.09	15–36	0.001*
POMS[e]	Tension/anxiety	5.98	0–20	6.62	0–20	0.025*
	Depression/dejection	3.54	0–20	4.18	0–20	0.008*
	Anger/hostility	2.69	0–18	3.32	0–18	0.001*
	Vigor/activity	8.22	0–20	8.01	0–20	0.243
	Fatigue/inertia	6.72	0–20	6.99	0–20	0.537
	Confusion/bewilderment	4.42	0–16	4.85	0–16	0.052

[a] The WHO subjective well-being inventory

[b] Positive affect

[c] Negative affect

[d] Raven's Advanced Progressive Matrix

[e] Profile of Mood States

Table 2. Distribution of SUBI[a] scores and association between PA[b] and NA[c]

	≤18	19–24	25–30	31–36	37–42	43–48	49–54	55–57	Mean	beta value, *t*-value, *p*-value
PA	1	6	112	354	479	234	23		37.90	(0.410, 15.525, 1.090×10^{-49})
NA		1	9	65	238	497	372	27	45.65	

Numbers in the table represent the number of subjects in each score range.

[a] The WHO subjective well-being inventory

[b] Positive affect

[c] Negative affect

Table 3. Associations between SUBI[a] score and psychological variables (RAPM[b] and POMS[c])

	PA[d]				NA[e]			
	β	t	*p* (uncorre	*p* (FD	β	t	*p* (uncorre	*p* (FD

				cted)				cted)	R)
RAPM		−0.029	−0.996	0.319	0.319	0.016	0.546	0.585	0.585
POMS	Tension/anxiety	−0.220	−7.865	8.181×10^{-15}	1.909×10^{-14}*	−0.374	−14.076	8.981×10^{-42}	3.14×10^{-41}*
	Depression/dejection	−0.271	−9.804	6.955×10^{-22}	2.434×10^{-21}*	−0.466	−18.349	1.643×10^{-66}	0×10^{-65}*
	Anger/hostility	−0.187	−6.625	5.206×10^{-11}	9.111×10^{-11}*	−0.350	−12.998	3.036×10^{-36}	5.31×10^{-36}*
	Vigor/activity	0.351	12.972	4.365×10^{-36}	3.055×10^{-35}*	0.168	5.911	4.445×10^{-9}	5.18×10^{-9}*
	Fatigue/inertia	−0.179	−6.302	4.143×10^{-36}	5.801×10^{-10}*	−0.354	−13.142	6.230×10^{-37}	1.45×10^{-36}*

				3.36						1.06
Confusion/bewil derment	−0.1 04	−3.6 36	2.884×10^{-4}	5×10^{-4} *	−0.3 24	−11. 881	7.609×10^{-31}	5×10^{-3} ^{0}*

* $p < 0.05$, corrected for multiple comparisons using false discovery rate

[a] The WHO subjective well-being inventory

[b] Raven's Advanced Progressive Matrix

[c] Profile of Mood States

[d] Positive affect

[e] Negative affect

[f] False discovery rate

Table 4. Brain regions with significant correlation between MD[a] and the SUBI[b] scores

	Gray matter areas included	Large bundles included	x	y	z	TFCE[c] value	Corrected *p*-value (FWE[d]-corrected, TFCE)	Cluster size (voxel)
Negative correlation	Right putamen/insula/pallidum/thalamus/caudate body	Right anterior limb of internal	33	−6	11	1232.09	0.026	1958

with PA[e] score		capsule/posterior limb of internal capsule/superior corona radiata/posterior corona radiata/external capsule					
Negative correlation with NA[f] score	Right putamen/thalamus/insula/pallidum/caudate body	Right posterior limb of internal capsule/posterior corona radiata/external capsule	24	0	2	1404.76	0.013	6354

Right middle cingulate gyrus	Right cingulum	14	−29	32	980.93	0.044	254

[a] Mean diffusivity

[b] The WHO subjective well-being inventory

[c] Threshold-free cluster enhancement

[d] Family-wise error

[e] Positive affect

[f] Negative affect

Table 5. Brain regions with significant correlation between FA[a] and SUBI[b] scores

	Large bundles included	x	y	z	TFCE[c] value	Corrected *p*-value (FWE[d]-corrected, TFCE)	Cluster size (voxel)
Negative correlation with NA[e] score	Right anterior limb of internal capsule	18	−1.5	13.5	412.66	0.044	32

[a] Fractional anisotropy

[b] The WHO subjective well-being inventory

[c] Threshold-free cluster enhancement

[d] Family-wise error (FWE)

[e] Negative affect

Supplementary methods

Preprocessing of imaging data

Segmentation of structural data

We adopted the two-step segmentation process for segmentation of diffusion images. First, fractional anisotropy (FA) images of each individual were segmented into six tissues using the new segmentation algorithm implemented in SPM8. Default parameters and tissue probability maps were used, except that affine regularization was performed using the International Consortium for Brain Mapping (ICBM) template for east Asian brains, and the sampling distance (the approximate distance between sampled points when estimating the model parameters) was 2 mm. Next, we synthesized the FA images and MD maps of each individual by following the procedures to create new images in which some parts were FA images and other parts were MD maps. In these synthesized images, the areas with a WM tissue probability of > 0.5 in the abovementioned first segmentation process was the FA image multiplied by −1; hence, this synthesized image shows a very clear contrast between the WM and other tissues, the remaining area was the MD map. The synthesized image from each individual was then segmented using the new segmentation with the same parameters as above. We adopted this two-step segmentation process due to the need to combine contrast information between WM and GM from FA images with the MD map, which alone does not show a clear contrast between WM and GM. For more details regarding this two-step segmentation process, see our previous study (Takeuchi *et al.*, 2013).

Normalization of structural data

After segmentation of the diffusion images, we proceeded with the diffeomorphic

anatomical registration through exponentiated lie algebra (DARTEL) registration process implemented in SPM8. In this process, the GM input for the DARTEL process was the DARTEL-imported image of the GM tissue probability map produced in the second new segmentation process. The WM input for the DARTEL process was created as follows. First, the raw FA images were multiplied by the WM tissue probability map produced in the second new segmentation process within the areas with a WM probability of > 0.5 (the signals from other areas were set to 0). The FA multiplied by the WM tissue probability map was used in the DARTEL procedures because this image includes different signal intensities within the WM tissues and improves accuracy of adjusting the image to the template from the perspective of not only the outer edge of the tissue, but also within WM tissues. Then, this FA multiplied by the WM tissue probability map was co-registered and resliced to the DARTEL-imported WM tissue probability map produced in the second new segmentation. The template for the DARTEL procedures was created using imaging data from 63 participants, who had been involved in a previous study (Takeuchi *et al*, 2011), and were also included in the present study. We used a template created from only a portion of participants as n = 63 is enough to create a template and thus cannot be considered to be problematic. Using this existing template, DARTEL procedures were performed on all of the subjects. In these DARTEL procedures, parameters were changed as follows to improve accuracy. The number of Gauss-Newton iterations to be performed within each outer iteration was set to 10 and, for each outer iteration, we used 8-fold more time points than the default to solve the partial differential equations. The number of cycles used by the full multi-grid matrix solver was set to 8. The number of relaxation iterations performed in each multi-grid cycle was set to 8. After running DARTEL, the resulting synthesized

images were spatially normalized to the MNI space. Using the parameters for these procedures, the raw MD map, raw FA map, GM segmentation map [GM concentration (density or segmentation) (GMC) map], WM segmentation map [WM concentration (density or segmentation) (WMC) map], and cerebral spinal fluid (CSF) segmentation map [CSF concentration (density or segmentation) (CSFC) map] from the abovementioned second new segmentation process were normalized to give images of $1.5 \times 1.5 \times 1.5$ mm^3. Subsequently, from the images of the normalized MD map, GMC map, WMC map, or CSFC map, areas that were not strongly likely to be gray or white matter (defined as "gray matter tissue probability + white matter tissue probability < 0.99") were removed to exclude the strong effects of CSF on MD. Whereas, from the normalized images of the FA, areas that were not strongly to be white matter (defined as "white matter tissue probability < 0.99") were removed. In these procedures, our custom template created from average images of the normalized GMC and the normalized WMC images of the abovementioned 63 participants were used. Then, MD images were smoothed by convolving them with an isotropic Gaussian kernel of 8-mm full width at half maximum (FWHM), and FA images with 6-mm FWHM. For more details regarding these normalization procedures, see our previous study (Takeuchi *et al.*, 2013).

ROI analyses

We employed three kinds of regions of interest (ROI) analyses in this study: ROI analysis of areas highlighted by whole brain statistical analyses, ROI analysis for left-sided areas symmetric to those observed in the results of whole brain statistical analysis, and ROI analysis for areas chosen based on *a priori* hypothesis that SWB

might be related to MD in regions associated with the dopaminergic system. In each analysis, results with a threshold *p*-value of <0.05 were considered statistically significant after correcting for the FDR using the classical one-stage method (Benjamini and Hochberg, 2000). For the last ROI analysis, we chose areas typically related to the dopaminergic pathways without significant correlation in the whole brain statistical analyses.

ROI analyses of the associations between MD and SUBI

After identifying the MD correlates of the SUBI, an ROI approach was employed to areas highlighted by the whole brain statistical analyses. As previously reported (Takeuc*hi et al*, 2017), such an ROI analysis can be used to determine whether areas related to the SUBI scores were affected by the extent of MD or GM, WM, and CSF. The areas included the right globus pallidus, right putamen, right caudate body, and right thalamus. All ROIs were constructed using the WFU PickAtlas Tool (http://fmri.wfubmc.edu/software/pickatlas) (Maldjian et al., 2003; Maldjian et al., 2004). The mask images of the ROIs, except for the right thalamus, were generated using the Brodmann area option in the PickAtlas tool, whereas those of the right thalamus were generated using the Talairach Daemon option. These mask images were resliced, the defining space for which was a normalized image from a patient. Subsequently, the mean MD, GMC, WMC, and CSFC values of these images were extracted from the normalized and unsmoothed images. To extract these values, we limited the areas to those that showed "gray matter tissue probability + white matter tissue probability >0.999" in the custom template mentioned above. ROIs after abovementioned processes are shown in Supplementary Figure 1a-d. The associations

were tested using multiple regression analysis. The dependent variable was the mean MD in one of the ROIs, and the independent variables comprised PA and NA scores, age, sex, and the mean GMC, WMC, and CSFC values of the ROI.

ROI analyses for the left-sided areas symmetric to those observed in the results of whole brain statistical analyses

We employed ROI approaches to left-sided areas symmetric to those included in the whole brain analyses to confirm the presence of left-right laterality effect of the MD in the ROIs in terms of the association with SUBI. The mask images of the ROIs were generated, and resliced, and the mean MD, GMC, WMC, and CSFC values of these mask images were extracted. Multiple regression analyses were conducted in the same manner described in the abovementioned ROI analyses.

ROI analyses of the correlations between SUBI and MD in the dopaminergic areas without significant correlation in the whole brain analyses

We employed ROI approaches for areas that are typically associated with the dopaminergic system and do not exhibit significant correlation with SUBI scores in the whole brain statistical analyses. The bilateral nucleus accumbens (NAcc), substantia nigra (SN), and the ventral tegmental area (VTA), which are associated with the dopaminergic system (Wise, 2004), were included. All ROIs were constructed using the WFU PickAtlas tool (http://fmri.wfubmc.edu/software/pickatlas) (Maldjian et al., 2003; Maldjian et al., 2004). The mask images of ROIs for the left and right SN were constructed using the Brodmann area option in the PickAtlas tool. The mask images for the left and right NAcc were constructed using the IBASPM71 option considering that

ROIs for the NAcc cannot be selected in the Brodmann area options. Furthermore, the mask image of the VTA was set to a $9 \times 9 \times 9$ mm^3 voxel with the center of x, y, z = 0, − 15, − 12, respectively (Tomasi and Volkow, 2014) because there were no options that included the established area. Then, we constructed the masks of the five ROIs. These mask images of ROIs were resliced and the defining during this procedure was a normalized image from a patient. Subsequently, the mean MD, GMC, WMC, and CSFC values of these mask images were extracted from the normalized and unsmoothed images following the abovementioned manner for ROI analyses. ROIs after abovementioned processes are shown in Supplementary Figure 1e-g. The associations were tested using multiple regression analyses. The dependent variable was the mean MD in one of the ROIs and the independent variables comprised SUBI-PA or SUBI-NA scores, age, sex, and the mean GMC, WMC, and CSFC values of each ROI.

Analyses of sex differences in the neural correlates of SUBI scores

To investigate the MD (or FA) correlates of SUBI scores between sexes, we used voxel-wise analysis of covariance (ANCOVA) with sex difference as a grouping factor (using the full factorial option of SPM8). ANCOVA for PA and NA were separately performed similarly to the multiple regression analyses described in the main text. In these analyses, age, RAPM score, TIV, and PA or NA scores were included as covariates. The covariates of age, RAPM score, and the PA or NA score were modeled to ensure each covariate had a unique relationship with MD (or FA) for each sex (using the interactions option in SPM8), thereby enabling an investigation of the effects of interaction between sex and each covariate. Correction for multiple comparisons was

performed using the same method used in the whole-brain multiple regression analyses.

Supplementary Results

ROI analyses for the areas highlighted by the whole brain statistical analyses

In accordance with the results of the whole brain analyses, the areas correlated with the SUBI scores included parts of the right putamen, globus pallidus, caudate body, and thalamus. We performed ROI analyses to investigate potential correlations between the MD of these areas and the SUBI-PA or SUBI-NA scores after correcting for confounding variables of the MRI data (GMC, WMC, and CSFC), age and sex. As shown in Supplementary Table 1, for each SUBI score, there were significant negative correlations between SUBI scores and MD in the right putamen, right globus pallidus, right caudate body, and right thalamus

ROI analyses for the left-sided areas symmetric to those observed in the whole brain statistical analyses

We performed ROI analyses for the left-sided areas symmetric to those included in the whole brain analyses. As shown in Supplementary Table 2, no significant correlations were found between SUBI scores and MD in the ROIs except for that between PA and MD in the left caudate body.

ROI analyses of the correlations between SUBI and MD in dopaminergic areas not significantly correlated in whole brain analyses

We performed ROI analyses to investigate whether there was any correlation between MD in areas related to the dopaminergic system that did not exhibit significant correlation in the whole brain statistical analyses and SUBI-PA or SUBI-NA score after correcting for confounding variables of age, sex, TIV, and RAPM score. As shown in Supplementary Table 3, no significant correlation was noted between SUBI scores and MD in any ROIs).

Sex differences in the neural correlates of SUBI scores

We found no significant effect of interaction between sex and PA or NA score on MD. Significant interactions between NA and sex on FA moderated by the contrasts of positive associations in males and negative associations in females were observed in the left frontal sub-gyral region (Supplementary Table 4, Supplementary Figure 2). No significant effect of interaction between sex and PA score on FA were observed.

Supplementary Discussion

ROI analyses of the correlations between SUBI and MD in the dopaminergic areas not significantly correlated in whole brain analyses

Supplementary ROI analyses showed that there were no significant correlations between SUBI scores and MD in the VTA, bilateral NAcc, and SN, which could be considered to

be typical dopaminergic areas. It is not yet understood why areas extending to the right putamen, globus pallidus, caudate, thalamus and insula in the dopaminergic system have particularly significant correlations in the SUBI. As mentioned in a previous review, there are possibilities that the smallness of the partial-volume effects of CSF or accumulation of iron can affect MD in these areas (Takeuchi and Kawashima, 2018).

Sex differences in the neural correlates of SUBI scores

There were significant effects of interaction between sex and NA on FA in the left frontal sub-gyral white matter, which connects the cortical and subcortical areas and is involved in various cognitive and emotional processes (Moretti and Signori, 2016). The integrity of this connection may be related to the behavioral results considering that males had significantly better states of SWB with respect to NA. However, because the mechanism and significance of this association is unclear, future investigations are warranted.

Supplementary references

Benjamini, Y., Hochberg, Y. (2000). On the Adaptive Control of the False Discovery Rate in Multiple Testing With Independent Statistics. *Journal of Educational and Behavioral Statistics*, **25**, 60–83

Maldjian, J.A., Laurienti, P.J., Burdette, J.H. (2004). Precentral gyrus discrepancy in electronic versions of the Talairach atlas. *NeuroImage*, **21**, 450–55

Maldjian, J.A., Laurienti, P.J., Kraft, R.A., et al. (2003). An automated method for neuroanatomic and cytoarchitectonic atlas-based interrogation of fMRI data sets.

NeuroImage, **19**, 1233–39

Moretti, R., Signori, R. (2016). Neural correlates for apathy: Frontal-prefrontal and parietal cortical- subcortical circuits. *Frontiers in Aging Neuroscience*, **8**

Takeuchi, H., Kawashima, R. (2018). Mean Diffusivity in the Dopaminergic System and Neural Differences Related to Dopaminergic System. *Current Neuropharmacology*, **16**, 460–74

Takeuchi, H., Taki, Y., Hashizume, H., et al. (2011). Cerebral blood flow during rest associates with general intelligence and creativity. *PLoS ONE*, **6**, 4–12

Takeuchi, H., Taki, Y., Sekiguchi, A., et al. (2017). Mean diffusivity of basal ganglia and thalamus specifically associated with motivational states among mood states. *Brain Structure and Function*, **222**, 1027–37

Takeuchi, H., Taki, Y., Thyreau, B., et al. (2013). White matter structures associated with empathizing and systemizing in young adults. *NeuroImage*, **77**, 222–36

Tomasi, D., Volkow, N.D. (2014). Functional connectivity of substantia nigra and ventral tegmental area: Maturation during adolescence and effects of ADHD. *Cerebral Cortex*, **24**, 935–44

Wise, R.A. (2004). Dopamine, learning and motivation. *Nature Reviews Neuroscience*, **5**, 483–94

Supplementary Table 1. Matrix of statistical results (beta values, *t*-values, and *p*-values) for the multiple regression analyses of SUBI[a] scores and MD[b] in ROIs[c], with the covariates of age, sex, mean GMC[d], mean WMC[e] and mean CSFC[f] values in each ROI

	PA[g]				NA[h]			
	β	*t*	*p* (uncorrected)	*p* (FDR[i])	β	*t*	*p* (uncorrected)	*p* (FDR)
Right putamen	−0.09	−3.232	1.263×10^{-3}	2.921×10^{-3}*	−0.077	−2.743	6.170×10^{-3}	2.792×10^{-3}*
Right globus pallidus	−0.089	−3.19	1.461×10^{-3}	2.921×10^{-3}*	−0.09	−3.203	1.396×10^{-3}	2.792×10^{-3}*
Right caudate body	−0.081	−2.915	3.623×10^{-3}	4.459×10^{-3}*	−0.075	−2.696	7.112×10^{-3}	7.112×10^{-3}*
Right thalamus	−0.078	−2.849	4.459×10^{-3}	4.459×10^{-3}*	−0.092	−3.329	8.969×10^{-4}	7.112×10^{-3}*

*$p < 0.05$, corrected for multiple comparisons using FDR

[a] WHO-subjective well-being inventory

[b] Mean diffusivity

[c] Regions of interest

[d] Gray matter concentration

[e] White matter concentration

[f] Cerebrospinal fluid concentration

[g] Positive affect

[h] Negative affect

[i] False discovery rate

Supplementary Table 2. **Matrix of statistical results (beta values, *t*-values, *p*-values) for the multiple regression analyses of SUBI[a] scores and MD[b] in ROI[c], for the left-sided areas symmetric to those observed in the results of whole brain statistical analyses, with the covariates of age, sex, mean GMC[d], mean WMC[e], and mean CSFC[f] values in each ROI**

	PA[g]				**NA[h]**			
	β	*t*	*p* (uncorrected)	*p* (FDR[i])	β	*t*	*p* (uncorrected)	*p* (FDR)
Left putamen	−0.038	−1.34	0.182	0.24	−0.050	−1.73	0.083	0.11
Left globus pallidus	−0.053	−1.83	0.067	0.13	−0.065	−2.26	0.024	0.10
Left caudate body	−0.074	−2.59	0.010	0.04*	−0.053	−1.85	0.065	0.11
Left thalamus	0.007	0.23	0.820	0.82	−0.037	−1.28	0.201	0.20

* $p < 0.05$, corrected for multiple comparisons using FDR

[a] WHO-subjective well-being inventory

[b] Mean diffusivity

[c] Regions of interest

[d] Gray matter concentration

[e] White matter concentration

[f] Cerebrospinal fluid concentration

[g] Positive affect

[h] Negative affect

[i] False discovery rate

Supplementary Table 3. **Matrix of statistical results (beta values, *t*-values, *p*-values) for the multiple regression analyses of SUBI[a] scores and MD[b] in ROI[c], with the covariates of age, sex, mean GMC[d], mean WMC[e], and mean CSFC[f] values in each ROI**

		PA[g]				NA[h]			
		β	*t*	*p* (uncorrected)	*p* (FDR[i])	β	*t*	*p* (uncorrected)	*p* (FDR)
SN[j]	L[k]	−0.041	−1.418	0.156	0.164	−0.033	−1.136	0.256	0.336
	R[l]	−0.055	−2.023	0.043	0.103	−0.04	−1.463	0.144	0.269
VTA[m]		−0.056	−1.945	0.052	0.103	− 0.079	−2.760	0.154	0.269
Nacc[n]	L	−0.054	−1.893	0.059	0.103	− 0.048	−1.661	0.097	0.269
	R	−0.049	−1.742	0.082	0.107	− 0.014	−0.478	0.633	0.665

[a] WHO-subjective well-being inventory

[b] Mean diffusivity

[c] Regions of interest

[d] Gray matter concentration

[e] White matter concentration

[f] Cerebrospinal fluid concentration

[g] Positive affect

[h] Negative affect

[i] False discovery rate

[j] Substantia nigra

[k] Left

[l] Right

[m] Ventral tegmental area

[n] Nucleus accumbens

Supplementary Table 4. Brain regions exhibiting significant effects of the interaction between SUBI-NA[a] scores and sex (moderated by positive correlation in males and negative correlation in females) on FA[b]

	x	y	z	TFCE[c] values	Corrected *p*-values (FWE[d]-corrected, TFCE)	Cluster size (voxel)
Left hemisphere, sub-gyral white matter	−19.5	−34.5	33	418.93	0.037	55

[a] Negative affect (NA) of the subjective well-being inventory (SUBI)

[b] Fractional anisotropy

[c] Threshold-free cluster enhancement

[d] Family-wise error (FWE)

Supplementary Figure 1.

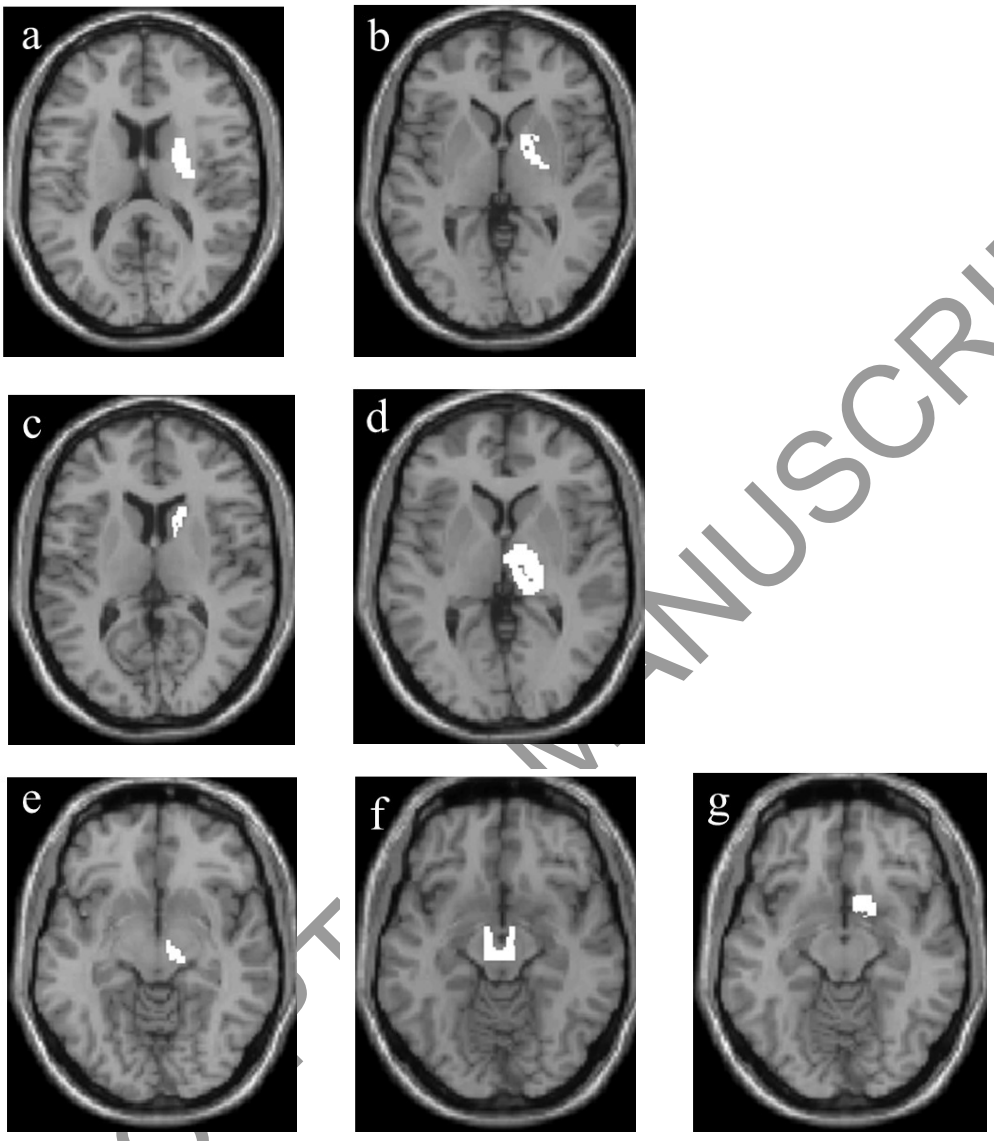

Supplementary Figure 2.

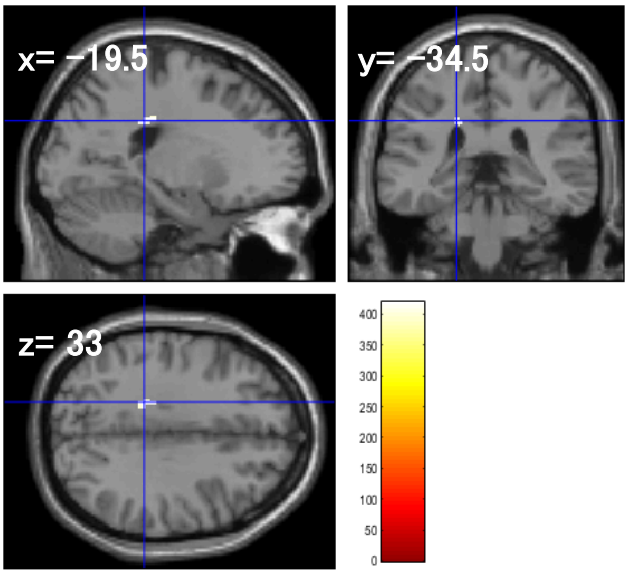

Figure legends

Supplementary Figure 1.

Brain regions exhibiting ROIs created in the supplementary methods and overlaid on a "single subject" T1 image in SPM8. These areas included (a) the right putamen, (b) right globus pallidus, (c) right caudate body, (d) right thalamus, (e) right substantia nigra, (f) ventral tegmental area, and (g) right nucleus accumbens.

Supplementary Figure 2.

Brain regions exhibiting significant effect of interaction between NA scores and sex (that are moderated by positive correlation in males and negative correlation in females) on FA. The result shown was obtained using threshold-free cluster enhancement (TFCE), $P < 0.05$ based on 5000 permutations. Regions with significant correlations are overlaid on a "single subject" T1 image in SPM8. The color represents the strength of the TFCE value. The significant interactions between NA and sex on FA that were moderated by the contrasts of positive associations in males and negative associations in females were found in the left frontal sub-gyral region.